Tactile Sensation Imaging for Artificial Palpation

Jong-Ha Lee[1], Chang-Hee Won[1], Kaiguo Yan[2], Yan Yu[2], and Lydia Liao[3]

[1]Control, Sensor, Network, and Perception (CSNAP) Laboratory, Temple University, Philadelphia, PA 19040, USA
{jong,cwon}@temple.edu
[2]Department of Radiation Oncology, Thomas Jefferson University Hospital, Philadelphia, PA 19107, USA
{kaiguo.yan,yan.yu}@jeffersonhospital.org
[3]Department of Radiology, Cooper University Hospital, Voorhees, NJ 08043, USA
{liao-lydia}@cooperhealth.edu

Abstract. In this paper we investigated a novel tactile sensation imaging method using a flexible, transparent waveguide and the total internal reflection principle. The developed sensor is used to detect and identify inclusions within tissues. To test the performance of the proposed sensor, a realistic tissue phantom with hard inclusions (tumor models) is developed. The proposed tactile imaging sensor estimated the inclusion diameter within 4.09% and the inclusion depth within 7.55%.

Key words: Tactile Sensation, Tactile Display, Haptic, Inclusion Detection

1 Introduction

Diagnosing early formation of tumors or lumps, particularly those caused by cancer, has been a challenging problem. To help physicians detect tumor more efficiently, various imaging techniques with different imaging modalities such as computer tomography, ultrasonic imaging, nuclear magnetic resonance imaging, and x-rays have been developed [1], [2]. However, each of these techniques has limitations, including the exposure to radiation, excessive costs, and complexity of machinery. Artificial tactile sensors are a valuable non-invasive tool for the medical society, where physicians use tactile sensation to identify malignant tissue [3], [4]. Traditionally physicians have used palpation to detect breast or prostate tumors, which is based on the observation that the tissue abnormalities are usually associated with localized changes in mechanical properties such as stiffness [5]. An artificial tactile sensor can accurately quantify and record the tactile sensation of benign and malignant regions.

In this paper, we present a newly designed tactile imaging sensor to detect or locate sub-surface inclusions such as tumors or lumps. Polydimethylsiloxane (PDMS) is used to make a multi-layer optical waveguide as a sensing probe. The mechanical properties of each layer have emulated the human finger layers to maximize the touch sensitivity. In our sensor, total internal reflection principle is utilized to obtain the high resolution of the tactile image. A force applied to an elastic waveguide, while light passes through it, causes change in the critical angle of internally reflected light. This results in diffused light outside the waveguide that is captured by a camera. The sensitivity and the resolution of the proposed sensor are controlled by the size of the waveguide and the light source intensity.

This paper is organized as follows: Section 2 discusses the proposed sensor design and sensing principle. Section 3 presents the experimental results for inclusion detection in a phantom. Finally, Section 4 presents the conclusions and discusses the future work.

2 Tactile Imaging Sensor Design and Sensing Principle

In this section, we present the design concept and sensing principle of the proposed sensor in detail.

2.1 Tactile Imaging Sensor Design

Fig. 1(a) shows the schematic of the tactile imaging sensor. The sensor comprises of an optical waveguide unit, a light source unit, a light coupling unit, a camera unit, and a computer unit.

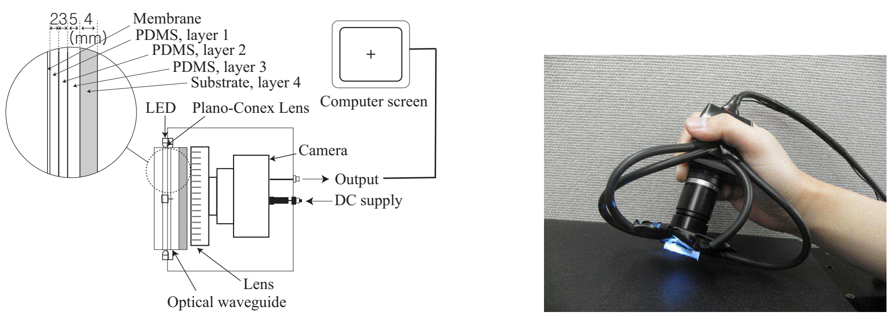

(a) (b)

Fig. 1. (a) The schematic of the tactile imaging sensor. (b) The tactile imaging sensor.

The optical waveguide is the main sensing probe. It is composed of three polydimethylsiloxane (PDMS, $Si(CH_3)_2$) layers, which is a high performance silicone elastomer [6]. The elastic modulus of each PDMS layer is matched as the modulus values of epidermis (1.4×10^5 Pa), dermis (8.0×10^4 Pa) and subcutanea (3.4×10^4 Pa) of a human fingertip to realize the sensitivity to the level of the human touch sensation [7]. The digital imager is a mono-cooled complementary camera with 4.65 μm $\times$ 4.65 μm individual pixel size. The maximum lens resolution is 1392 μm (H) $\times$ 1042 μm (V) with 60^o view angle. The camera is placed below an optical waveguide. A borosilicate glass plate is placed as a substrate between camera and optical waveguide to sustain the waveguide without losing camera resolution. The glass plate emulates the bone in the human fingertip. The internal light source is a micro-LED with a diameter of 1.8 mm. There are four LEDs used on four sides of the waveguide to provide enough illumination. The direction and incident angle of the LED light have been calibrated with the acceptance angle and it is discussed in the next section. Fig. 1(b) shows the integrated tactile imaging sensor.

2.2 Sensing Principle

The tactile imaging sensor is developed based on the optical phenomenon known as the total internal reflection (TIR) principle of light in a multi-layer optical waveguide. To maintain the light in a waveguide, the critical angle and the acceptance angle of light are analyzed using the geometric optics approximation. This allows determining the direction of the light source illumination.

Consider light trapped inside the multi-layer waveguide in the geometry as shown in Fig. 2. As a result of Snell's Law, the light propagation angle γ_i, $i = 0, 1, 2, 3, 4$ are bound by the following relations:

$$n_{i+1} \sin \gamma_{i+1} = n_i \sin \gamma_i, \tag{1}$$

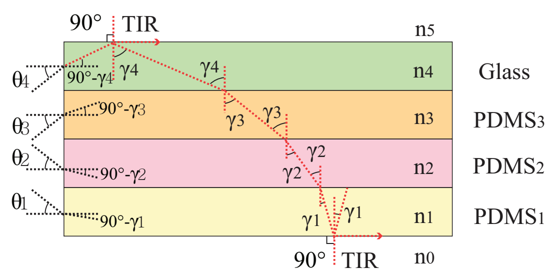

Fig. 2. Graphic representation of light propagation as a ray, propagating in the waveguide.

Here n_0 and n_5 are the refractive indices of air $n_0 = n_5 = 1$. The critical TIR angles γ_1 and γ_4 are achieved when $\gamma_0 = \gamma_5 = 90^o$ at the boundaries with air. Light propagating in the waveguide with angles γ_1, γ_2, γ_3, γ_4 or higher in their respective layers will remain trapped inside the waveguide. The critical angle indicates the minimum propagation angle. To make the propagation angle above the critical angle, the acceptance angle of light source has been calculated.

The acceptance angle θ_i is the maximum angle, under which the light directed into the waveguide remains trapped inside it. The propagation angle γ_i are related to the acceptance angle θ_i by the same Snell's law:

$$\sin \theta_i = n_i \sin(90^o - \gamma_i) = n_i \cos \gamma_i. \tag{2}$$

Further, transforming Eq. (2), we obtain

$$\sin\theta_i = n_i \cos\gamma_i = n_i(1-\sin^2\gamma_i)^{1/2} = (n_i^2 - n_i^2\sin^2\gamma_i)^{1/2}. \quad (3)$$

But as follows from Eq. (1), all $n_i \sin\gamma_i$ are equal to n_0, which is equal to 1 for air. Therefore, we finally have

$$\theta_i = \mathrm{asin}[(\mathrm{n}_i^2 - 1)^{1/2}]. \quad (4)$$

Light, incident on layer i under the acceptance angle θ_i, will be trapped inside the waveguide.

In the current design, the refractive index of each PDMS layer and glass plate are measured approximately as 1.41, 1.40, 1.39, 1.38 and the acceptance angles θ_i are calculated as $\theta_1 = 83.73^o$, $\theta_2 = 78.46^o$, $\theta_3 = 74.89^o$, and $\theta_4 = 71.98^o$. Thus for the TIR in the waveguide, the spatial radiation pattern of LED light with the angle less than $71.98^o \times 2 = 143.96^o$ has been chosen and placed to inject the light.

3 Inclusion Detection Experiments

In this section, we performed the inclusion detection experiments using the tactile imaging sensor.

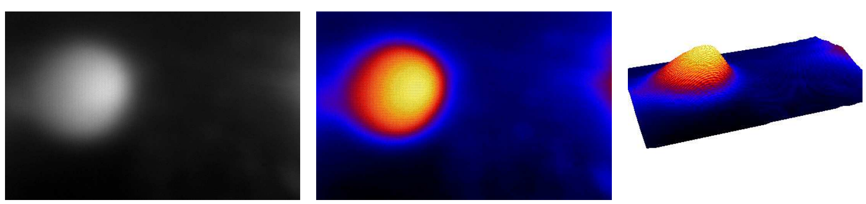

(a) (b) (c)

Fig. 3. The tactile image of inclusion with 3.29 diameter placed at the 4.2 mm depth. (a) Grey scale tactile image, (b) Color visualization, (c) 3-D reconstruction.

3.1 Empirical Equation of Inclusion Characterization

For the experiments, a tissue phantom with embedded hard inclusions (simulated tumor) has been developed. The phantom was made of a silicone composite having Young's modulus of approximately $5 \sim 10$kPa. To find the relation between tactile image and inclusion size, total of nine inclusions with different diameters were placed below the surface of the phantom. The inclusion was made using another silicone composite, the stiffness of which was much higher ($300 \sim 500$kPa) than the surrounding tissue phantom. The depth of each inclusion was 4.2 mm. To find the relation between tactile image and inclusion depth, eight inclusions were placed in the tissue phantom with varying depth. The diameter of each inclusion was 5.15 mm. The tactile images of each inclusion were obtained under the normal force of between 10 mN and 20 mN.

Fig. 3 shows a sample tactile image of inclusion with 3.29 mm diameter placed at the 4.2 mm depth. Figs. 4(a) and 4(b) represent the integrated pixel value of tactile images along the diameter and depth of the inclusions. The curve fitting method was used with these empirical measurements.

$$P_1 = (1.0 \times 10^7)[1.0 \times 10^{-3} D + 1.21], \tag{5}$$

$$P_2 = (-1.0 \times 10^7)[4.1 \times 10^{-2} H - 2.06]. \tag{6}$$

where D is the inclusion diameter and H is the inclusion depth. P_1 and P_2 are the integrated pixel value for different inclusion diameter D and depth H. Eqs. (5) and (6) will vary with the thickness and the modulus of the surrounding tissue sample.

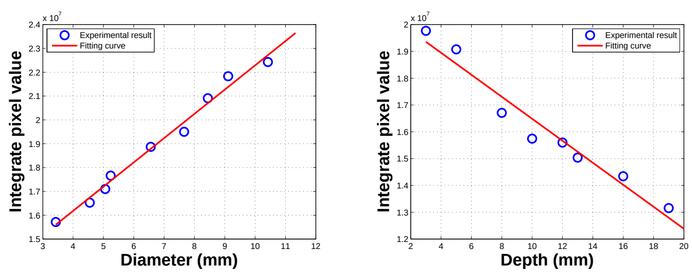

(a) (b)

Fig. 4. (a) Diameter versus integrated pixel value of tactile image. (b) Depth versus integrated pixel value of tactile image.

3.2 Inclusion Diameter and Depth Estimation

The inclusion parameter estimations (i.e. diameter and depth) based on the obtained tactile image can be formulated as an inversion problem. In our case, the integrated pixel value of tactile image is taken as input for the problem. For the inclusion diameter estimation experiments, two new inclusions were embedded into the tissue with the same depths of 4.2 mm. After obtaining the tactile images, the diameters have been estimated using Eq. (5). Similarly, for the depth estimation experiments, another two inclusions with the same diameters of 5.15 mm have been embedded and the depths have been estimated using Eq. (6). The results are shown in Table 1 and 2. The tactile imaging sensor estimated the inclusion diameter within 4.09% and the inclusion depth within 7.55%. So far we have determined either the diameter or the depth of the inclusions. The next step is to determine both diameter and depth based on one tactile image.

Table 1. Inclusion Diameter Estimation.

	Truth	**Estimate**	**Error**
Inclusion 1	4.91 mm	4.76 mm	3.05 %
Inclusion 2	6.35 mm	6.61 mm	4.09 %

Table 2. Inclusion Depth Estimation.

	Truth	**Estimate**	**Error**
Inclusion 3	9.01 mm	9.59 mm	7.55 %
Inclusion 4	15.11 mm	14.71 mm	2.65 %

4 Conclusions

In this paper, a new tactile sensation imaging method for artificial palpation is proposed and experimentally evaluated. To increase the sensitivity of touch, an optical waveguide consisting of three different elastic moduli of PDMS is fabricated as the sensing probe. The experimental results show that the proposed sensor successfully identifies inclusion diameter and depth from the tactile images.

References

1. Sojaku, H., Seto, H., Iwai, H., Kitazawa, S., Fukushima, W., Saito, K.: Detection of Incidental Breast Tumors by Noncontrast Spiral Computed Tomography of the Chest. Radiat. Med. 3, 780–782 (2008)
2. Gentle, C.R.: Mammobarography: A Possible Method of Mass Breast Screening. J. Biomech. Eng. 10, 124–126 (1998)
3. Wellman, P.S., Dalton, E.P., Krag, D., Kern, K.A., Howe, R.D.: Tactile Imaging of Breast Masses. Arch. Sur. 136, 204–208 (2001)
4. Howe, R.D., Matsuoka, Y.: Robotics for Surgery. Annual Review of Biomedical Engineering. 1, 211–240 (1999)
5. Krouskop, T.A., Wheeler, T.B., Kallel, F., Garra, B.S., Hall, T.: Elastic Moduli of Breast and Prostate Tissues under Compression. Ultrason. Imaging. 20, 260–274 (1998)
6. Chang-Yen, D.A., Eich, R.K., Gale, B.K.: A Monolithic PDMS Waveguide System Fabricated using Soft-lithography Techniques. J. Light. Tech. 23, 2088–2093 (2005)
7. Kandel, E., Schwartz, J., Jessell, T.: Principles of Neural Science. McGraw-Hill Medical (2000)